

Quasar feedback: accelerated star formation and chaotic accretion

Sergei Nayakshin and Kastytis Zubovas

Department of Physics & Astronomy, University of Leicester, Leicester, LE1 7RH, UK

E-mail: Sergei.Nayakshin@astro.le.ac.uk

Received

ABSTRACT

Growing Supermassive Black Holes (SMBH) are believed to influence their parent galaxies in a negative way, terminating their growth by ejecting gas out before it could turn into stars. Here we present some of the most sophisticated SMBH feedback simulations to date showing that quasar’s effects on galaxies are not always negative. We find that when the ambient shocked gas cools rapidly, the shocked gas is compressed into thin cold dense shells, filaments and clumps. Driving these high density features out is much more difficult than analytical models predict since dense filaments are resilient to the feedback. However, in this regime quasars have another way of affecting the host – by triggering a massive star formation burst in the cold gas by over-pressurising it. Under these conditions SMBHs actually accelerate star formation in the host, having a positive rather than negative effect on their host galaxies. The relationship between SMBH and galaxies is thus even more complex and symbiotic than currently believed. We also suggest that the instabilities found here may encourage the chaotic AGN feeding mode.

1 INTRODUCTION

Several properties of galaxies correlate with the mass of SMBHs residing in their centres (Tremaine et al. 2002; Häring & Rix 2004; Cattaneo et al. 2009), suggesting a causal link. These relations are currently attributed to the appreciable destructive powers of quasars (Silk & Rees 1998; Zubovas & King 2012). At high SMBH accretion rates, quasars launch wide angle outflows with velocity of $v_{\text{out}} \sim 0.1c$ as observed (Pounds et al. 2003b,a; Tombesi et al. 2010) in AGN X-ray absorption spectra, capable of ejecting all the gas from the host galaxy (Silk & Rees 1998; Zubovas & King 2012). Analytical arguments (King 2003) set the momentum-driven critical SMBH mass limit, M_σ , that closely matches the observed correlations (Tremaine et al. 2002; Häring & Rix 2004; Cattaneo et al. 2009). However how the outflow expels the gas is not clear in detail: previous analytical models include the essential outflow physics but assume spherical symmetry; numerical models are 3D but physically over-simplified due to computational constraints (Di Matteo et al. 2005; Sijacki et al. 2007; Booth & Schaye 2009).

As any fast outflow from a point source, the quasar outflow leads to two shocks, one inner – the shocked SMBH outflow itself – and the other outer, representing the shocked host galaxy gas. The two shocks are separated by a contact discontinuity (see fig. 1 in Zubovas & King 2012). Previous work has shown that the radiative cooling of the inner shock has a profound effect on the ability of the SMBH to drive the gas out of host galaxies. If the radiative time of

the inner shock is short, only the momentum from the primary quasar outflow is efficient in affecting the host gas, with the mechanical energy lost to radiation (King 2003). When the cooling time is long, the mechanical energy of the outflow thermalises (King 2005) and increases the hot gas pressure inside the quasar-driven bubble, leading to an even more powerful and rapid $v \sim 1000 \text{ km s}^{-1}$ outflow (Zubovas & King 2012).

Here we present numerical simulations that combine the strengths of the previous analytical (detailed feedback physics) and numerical (3D geometry) methods. Our simulations show that the way in which quasar outflows affect the gas in the host galaxies also strongly depends on whether the *outer* shock rapidly cools radiatively or not. In the former case, the shocked outer layer is very dense and is unstable to the “thin shell” instabilities previously known from supernova remnant studies (Vishniac 1983; Mac Low et al. 1989). These instabilities lead to the shell breaking up into thin dense filaments that are resilient to the outward push from the quasar outflow but are susceptible to a triggered (or at least accelerated) star formation. We propose that the latter process may constitute a positive quasar feedback effect on their host galaxies. Below we detail where and when this effect may be important.

2 MODEL AND NUMERICAL METHODS

Due to computational limitations, sub-grid models are a necessity to describe SMBH feedback in simulations that span cosmologically interesting volumes. Depositing energy

arXiv:1207.7200v1 [astro-ph.CO] 31 Jul 2012

into the gas nearest to SMBH (e.g., SPH particle neighbours of the SMBH) is the most widely used method (Di Matteo et al. 2005; Sijacki et al. 2007; Booth & Schaye 2009) for such simulations. In this paper we study AGN feedback on scales of a single galactic bulge, and therefore we can afford (a) a much higher numerical resolution and (b) a more detailed physical model for AGN feedback. The outflow physics follows the King (2003, 2005); King et al. (2011) model (cf. §2.1 in Zubovas & Nayakshin 2012) while the numerical method follows Zubovas & Nayakshin (2012) exactly (see their §3.1), except for different initial conditions. In brief, hydrodynamics of gas in the host galaxy and gravity solvers are based on code *Gadget* (Springel 2005). In contrast to the nearest neighbour method for AGN feedback, we model the propagation of fast ($v_{\text{out}} = 0.1c$) outflow from the SMBH explicitly via “virtual particles” introduced by Nayakshin et al. (2009). These particles are emitted isotropically by the SMBH, and propagate radially outward with no self-interaction allowed. SPH density field is continuously calculated at the particles’ instantaneous locations, and the interaction with an SPH particle occurs only when the latter contains the virtual particle within its SPH smoothing kernel. The method has been shown (Nayakshin & Power 2010) to reproduce analytical results of King (2003, 2005), and has been compared with the nearest neighbours feedback method by Power et al. (2011). Zubovas & Nayakshin (2012) further included optically thin photo-ionisation and inverse Compton heating of the galaxy’s gas by the quasar radiation field (Sazonov et al. 2005); this heating may be an important feedback effect in gas-poor epochs (e.g., Ciotti & Ostriker 2007).

Additionally, not only the momentum but also a fraction $g_E = \exp[-R_{\text{ic}}/R]$ of the virtual particles’ mechanical energy is passed to the ambient SPH particles, where $R_{\text{ic}} \approx 0.5$ kpc (for the parameters chosen below) is the inner shock cooling radius of the inner AGN outflow shock (King 2003, 2005). This radius is not to be confused with the outer shock cooling radius, R_{oc} , introduced later in the Discussion section of the paper. Note that $g_E(R \ll R_{\text{ic}}) \rightarrow 0$, while $g_E(R \gg R_{\text{ic}}) \rightarrow 1$. This energy deposition prescription mimics the transition from the radiatively efficient inner shock regime (small radii), when only the momentum of the SMBH outflow is passed to the gas, and the radiatively inefficient regime (large radii), when both energy and momentum are available to drive the host’s gas out (see King et al. 2011). Faucher-Giguère & Quataert (2012) have recently noted that if ions decouple thermally from electrons in the inner shock then the radiative cooling becomes far less efficient than obtained with a one-temperature model for the shock. The inner cooling radius R_{ic} in this case is negligibly small. We note that this (if correct) would introduce quantitative but not qualitative changes to our main results below, as we experimented with shells initially much smaller and also much larger than R_{oc} (to be reported elsewhere).

To demonstrate our points as clearly as possible, the host galaxy is modelled here by a fixed singular isothermal sphere potential softened at the centre where the SMBH is located. The ambient gas is initialised as a sphere with inner radius R_{in} and outer radius $R_{\text{out}} = 10R_{\text{in}}$, at rest, and with the density profile given by

$$\rho_g(R) = f_g \rho_0(R) = \frac{f_g \sigma^2}{2\pi G R^2}, \quad (1)$$

with $\rho_g(R) = 0$ for $R < R_{\text{in}}$ and $R > R_{\text{out}}$; here $\sigma = 141 \text{ km s}^{-1}$ is the velocity dispersion of the potential, $f_g = 0.16f$ is the gas ratio of the gas density to the underlying density of stars and dark matter; $f > 0$ is a free parameter. Initial gas temperature is set such that the sound speed is equal to σ . At time $t = 0$, the quasar outflow is turned on. The critical M_σ mass above which the SMBH outflow should expel the gas for this potential (Nayakshin & Power 2010) is $M_\sigma \approx 1.5 \times 10^8 f M_\odot$.

We fix the quasar momentum outflow rate and the SMBH mass in order to avoid model-dependent complications near SMBH. To avoid increasingly short time-steps at small radii, we use the accretion radius approach (Power et al. 2011) and remove SPH particles from the simulation that are closer than 30 pc from the SMBH. The densest and coldest self-gravitationally bound regions would continue to contract to arbitrarily large densities, a process which physically terminates in star formation. When gas density exceeds 200 times the potential’s tidal density ρ_0 , and the Jeans mass in the clump is smaller than the SPH kernel (40 particle neighbours) mass, SPH particles are turned into collisionless star particles. Our treatment of star formation neglects feedback effects from massive stars; this does not alter our main conclusions.

3 RESULTS FOR SPHERICAL SHELLS

We first present two simulations that exemplify the effects of the quasar outflow on the host galaxy’s gas in two extremes, e.g., (i) when the shocked gas can cool rapidly and (ii) when radiative cooling is inefficient (low gas density).

3.1 Thin shell instabilities

Figure 1 shows the density (left column) and temperature (right column) of the ambient gas shocked by the outflow in simulation F1 in the gas-rich epoch ($f = 1$, top panels), and in simulation F0.03, corresponding to a gas-poor epoch regime ($f = 0.03$, bottom panels). For both simulations, the SMBH mass is $M_{\text{bh}} = 10^8 M_\odot$ and the outer shell radius is $R_{\text{out}} = 2$ kpc. The host galaxy is rapidly emptied of gas in F0.03; the shock front velocity is about 1500 km s^{-1} , so that the shock expanded to $R \sim 1$ kpc by the time of the snapshot, $t = 0.57$ Myr. In contrast to that, the same SMBH outflow in the gas-rich simulation F1 stalls: the radius of the shock front is $R \sim 0.4$ kpc at time $t = 3.8$ Myr. This immense difference is due to two factors, both significant here: (i) the weight of the gas larger by a factor of ≈ 30 in F1 than in F0.03, and (ii) the inner shock remains in the momentum driven regime in F1, since the shell stalls at $R < R_{\text{oc}}$, whereas the shock becomes non-radiative and thus energy driven in simulation F0.03. These results are consistent with the analytical expectations for spherically symmetric shells (Zubovas & King 2012).

An unexpected result is that while the shocked shell is quasi-spherically symmetric in F0.03, it goes violently unstable in F1. In hindsight, the result is completely analogous to the stability of supernova remnant shells. *Cold* dense swept-up shells are strongly unstable to Rayleigh-Taylor and Vishniac (1983) instabilities (Mac Low et al. 1989), whereas *non-radiative hot and geometrically thick* shocks are stable

(compare fig. 3 in Mac Low et al. (1989) with the rest of their figures). Physically, radiative cooling is key for development of the instabilities because any initial density inhomogeneities are amplified when denser regions cool and get compressed by the high pressure surroundings; without cooling these density inhomogeneities tend to diffuse away.

The cold dense filaments are crucial to understanding of SMBH feedback on host galaxies and also the SMBH feeding, as we shall see.

3.2 Accelerated star formation

The cold dense filaments in simulation F1 are the birth place for newly born stars. The right panel of Figure 2 presents the gas temperature projected along rays as seen from the SMBH for simulation F1. The shell is a web of cold dense filaments with the strongest density peaks occurring at filament intersections. The left panel of the figure shows the density and velocity field at the time when dense filaments are starting to fall inward. Stars (red or cyan dots) are born inside the densest and coldest filaments.

Physically, quasar shocks are able to trigger star formation, or accelerate it, by compressing the cold gas in the hosts because the pressure produced by the quasar outflow is far higher than the maximum gas pressure inside the pre-quasar host, $P_{\max} \sim f_g \rho_0 \sigma^2$ (if the gas were hotter, $c_s^2 > \sigma^2$, a thermal pressure-driven wind would result). The pressure in the shocked ambient gas and inside the hot bubble inflated by the quasar is $P_{\text{sh}} \sim f_g \rho_0 v_e^2$, where $v_e \gg \sigma$ is the energy-driven shell expansion velocity calculated in King et al. (2011). In the energy-driven regime, the quasar's bubble pressure is higher than P_{\max} by the ratio

$$\frac{P_{\text{sh}}}{P_d} = \left(\frac{v_e}{\sigma}\right)^2 \sim 24 \sigma_{150}^{-2/3} f^{-2/3} \gg 1. \quad (2)$$

To exemplify the quasar's ability to trigger star formation further, consider the effects of the quasar outflow on a starburst gas disc. Such discs may have star formation rates as high as $\sim 10^3 \text{ M}_\odot \text{ yr}^{-1}$ while self-limiting their star formation rates (Thompson et al. 2005) by star formation feedback. Their midplane pressure is $P_d \sim \rho_0 \sigma^2 f_d^2$, where $f_d < f_g$ is the disc mass fraction at a given R . This is smaller than P_{\max} , so we see that even the starburst-supported discs are compressed to higher densities by quasar outflows. Since star formation rates are proportional to P_d in these discs (Thompson et al. 2005), disc compression due to quasar shock results in an even faster starburst in the disc.

3.3 Chaos and order in SMBH accretion

SMBH accretion is still far from understood. One of the significant challenges is the “star formation catastrophe” of self-gravitating parsec scale discs (Paczynski 1978; Nayakshin et al. 2007) in which gas is consumed more rapidly in star formation than it is fed to the SMBH. One proposed solution is disc self-regulation (Goodman 2003), and the other is “chaotic accretion”, in which angular momentum of gas is cancelled in shocks rather than transferred away (King & Pringle 2006). Chaotic SMBH feeding is suggested to encourage a more rapid SMBH growth in the early Universe (King & Pringle 2006) by limiting SMBH spin and may also explain (Nayakshin et al. 2012)

why SMBH do *not* correlate well with properties of galactic discs (Kormendy et al. 2011). Such flows could develop as a result of messy initial conditions or supernova-driven turbulence in the bulge (Hobbs et al. 2011).

Thin shell instabilities (Vishniac 1983), re-discovered here in the SMBH growth context, are thus an additional way of developing such multi-phase chaotic inflows *starting from non-turbulent spherically symmetric* initial conditions. The resulting gas flows are indeed highly variable as infalling fingers (see figure 2) shadow the ambient gas in an unpredictable way. On the other hand, if the ambient gas possesses symmetry before SMBH feedback is turned on, then there may be preferred inflow directions and an orderly flow/outflow develops in this case: for example, see simulations by Zubovas & Nayakshin (2012) for the *Fermi Bubbles* in the centre of the Milky Way. Further simulations with a range of realistic initial conditions are needed to investigate the importance of chaotic inflows for SMBH feeding.

4 IMPLICATION FOR NON-SPHERICAL GEOMETRIES

Having investigated an initially spherically symmetric shell in §3, we now wish to ask what happens in a more realistic case. Based on the earlier results, we expect that deviations from spherical symmetry in initial conditions will be amplified by the thin shell instabilities when the ambient shocked gas is able to cool rapidly. As before, the flow may break into dense inflowing and lower density outflowing regions or directions. If angular momentum is important then the denser flows may settle into a circularised disc.

We wish to emphasise the fact that the cooling rate of the shocked ambient gas is key to this behaviour. Figure 3 presents two contrasting simulations with same initial conditions but with ambient gas radiative cooling either on (left panel) or off (middle panel). The initial conditions are obtained from the spherical shell used in F1 by a linear transformation $z \rightarrow z/2$ which obviously makes an elliptical rather than a spherical initial shell. The shell also slowly rotates, $v_{\text{rot}} = 0.3 v_{\text{circ}}$, where $v_{\text{circ}} = 2^{1/2} \sigma$ is the circular velocity for the potential, with the angular momentum vector pointing in the positive z direction. Finally, the SMBH mass is slightly increased to $M_{\text{bh}} = 1.5 \times 10^8 \text{ M}_\odot$, the M_σ mass for this potential.

The left panel of Figure 3 shows that the outflow is channelled along the symmetry axis. However, as the ambient gas cools, most of it collapses onto the symmetry plane, becoming resilient to feedback and instead mainly turning into stars. This is in a stark contrast to a simulation shown in the middle panel of the same figure, where the radiative cooling in the ambient gas is artificially turned off. All of the gas is expelled in this case because the shocked ambient gas remains *hot* and always presents a large enough surface area for the SMBH feedback to work on.

To quantify this cooling-regulated behaviour, we introduced a free parameter $A_{\text{cool}} \geq 1$, which is used to artificially reduce the radiative cooling rate function $\Lambda \rightarrow \Lambda/A_{\text{cool}}$ in a set of numerical experiments which share same initial conditions as explained above. The left panel of Figure 3 corresponds to $A_{\text{cool}} = 1$, e.g., the proper unmodified cooling rate, whereas the middle panel of the figure corresponds to

$A_{\text{cool}} = \infty$ (e.g., cooling in the ambient gas is turned off). The right panel of figure 3 shows the fractions of gas expelled and turned into stars as functions of A_{cool} . We see that quasar outflows mainly turn gas into stars when the shocked gas cools rapidly but is able to expel most or even all of the gas if the shocked gas is unable to cool (large A_{cool}).

5 DISCUSSION

We presented simulations of the interaction between the fast outflow emanating from a quasar and the ambient gas in the host galaxy utilising the virtual particle method of Nayakshin et al. (2009). We believe the method is an improvement (see also Power et al. 2011) on the sub-grid nearest-particle methods since the SMBH outflow is explicitly modelled to track where and how it impacts the ambient gas, and whether the outflow’s momentum, energy, or both are passed to the ambient gas. In particular, consider the left panel of figure 2. The cold filaments subtend a small solid angle as seen from the quasar location and should thus encounter a small fraction of the quasar outflow only, with most quasar feedback impacting on the low density gas instead. This is correctly captured by our virtual particle method. In contrast, the nearest neighbour methods may spread *all of the quasar feedback energy* to the cold filaments because they tend to be closer to the SMBH.

Our key new result is the finding that the response of the ambient gas to the fast outflow of gas from the quasar depends critically on whether the ambient gas is able to cool rapidly or not. Generally, in the latter case the analytical criteria, such as the outflow momentum (thrust) balanced against the weight of the gas in the bulge are sufficient to establish whether the shell is driven outward, stalls or collapses (King 2003, 2005; King et al. 2011). However, when the outer shock is radiative, even initially spherically symmetric shells develop a multi-phase structure. Denser regions cannot be driven outward easily. Quasar outflows affect these high density regions most effectively not by expelling them outward but by compressing them and triggering (or at least accelerating) star formation there.

Let us now quantify the conditions when the ambient shocked gas is able to cool rapidly. Bremsstrahlung is the most significant cooling function for the problem at hand, with $\Lambda(T) = \Lambda_0 T^{1/2}$, $\Lambda_0 = 3.8 \times 10^{-27} \text{ erg cm}^3 \text{ s}^{-1}$. The shocked gas cooling time, $t_{\text{cool}} = 3kT/n\Lambda(T)$, where n and T is the shocked gas electron density and temperature, respectively. In the strong shock limit, $n = 4\rho_g(R)/(\mu m_p)$, where $\mu = 0.63$ is the mean molecular weight and $\rho_g(R)$ is the pre-shock gas density given by equation 1, and $T = (3/16)\mu m_p v_e^2/k_B$. To determine whether the quasar shock is radiative or adiabatic, t_{cool} should be compared with the shocked shell flow time scale, R/\dot{R} , where $\dot{R} = (4/3)v_e$ is the outer shock velocity (Zubovas & King 2012):

$$\frac{t_{\text{cool}}}{R/\dot{R}} = 0.83 \frac{3.8 \times 10^{-27}}{\Lambda_0} f^{-5/3} \sigma_{150}^{-2/3} \left(\frac{M_{\text{bh}}}{M_\sigma} \right)^{2/3} R_{\text{kpc}}. \quad (3)$$

At a fixed fraction f , the “outer cooling radius”, R_{oc} , the radius which separates the rapidly cooling outer shock regime from the slowly cooling one, can be defined by requiring that the ratio in equation 3 be equal to one. The result is:

$$R_{\text{oc}} = 1.2 \text{ kpc } f^{5/3} \sigma_{150}^{2/3} \left(\frac{M_\sigma}{M_{\text{bh}}} \right)^{2/3} \frac{\Lambda_0}{3.8 \times 10^{-27}}. \quad (4)$$

In the early gas rich epochs (which we operationally define as $f > 1$) SMBHs affect their hosts both positively via accelerating star bursts at “small” radii (at $R \lesssim R_{\text{oc}}$), and negatively at larger radii where the gas is more likely to be blown out. Interestingly, the powerful starbursts in submillimeter galaxies (e.g., galaxies forming stars at rates as high as $\sim 10^3 M_\odot \text{ yr}^{-1}$ at redshift $z \sim 2$) have been resolved by Tacconi et al. (2006) to have intrinsic sizes of a few kpc, comparable to R_{oc} in the gas-rich epoch.

In the later gas-poor epochs, when $f \ll 1$ everywhere, and $M_{\text{bh}} \gtrsim M_\sigma$, it follows from equation 4 that $R_{\text{oc}} \ll 1 \text{ kpc}$, so that shocked gas is unlikely to clump up into high density features over most of the observationally interesting scales in the host galaxy. In this regime quasars should be better able to sweep the hosts clear of gas if they are activated for long enough. This is the widely appreciated negative quasar/AGN feedback mode, and it probably explains why the present day ellipticals are “red and dead” and why their SMBHs are not very bright (Schawinski et al. 2009).

6 CONCLUSIONS

Our results broaden the spectrum of possible effects that SMBHs have on their host galaxies, showing that it is not all about ejecting the gas out. We found that it is increasingly difficult to drive gas out of the hosts at small radii, $R < R_{\text{oc}}$ (equation 4), in the early gas-rich epoch. Even in an initial spherical symmetry the thin and dense outer shell breaks into filaments and clumps that are hard to drive away but which can be readily over-pressurised by the hot quasar wind and which result in enhanced star formation rates. The latter process is a form of positive rather than negative AGN feedback on host galaxies (we note that similar statements were already made by Silk & Norman 2009, based on their analytical arguments). Non-spherical initial shell geometries only strengthen these conclusions as the multi-phase inflow-outflow separation becomes even more robust (see §4).

We also found that in later gas-poor epochs, when the shocked host’s gas cannot cool rapidly (cf. Discussion), the inhomogeneities do not develop (cf. the bottom panel of fig. 1) or do not grow for non-spherical initial conditions (cf. figure 3, the middle panel). The SMBH is then an efficient negative feedback engine as has been appreciated for a long time now.

7 ACKNOWLEDGMENTS

Andrew King is thanked for helpful comments and encouragement. Theoretical astrophysics research at the University of Leicester is supported by a STFC Rolling grant. This research used the ALICE High Performance Computing Facility at the University of Leicester. Some resources on ALICE form part of the DiRAC Facility jointly funded by STFC and the Large Facilities Capital Fund of BIS.

REFERENCES

Booth C. M., Schaye J., 2009, MNRAS, 398, 53

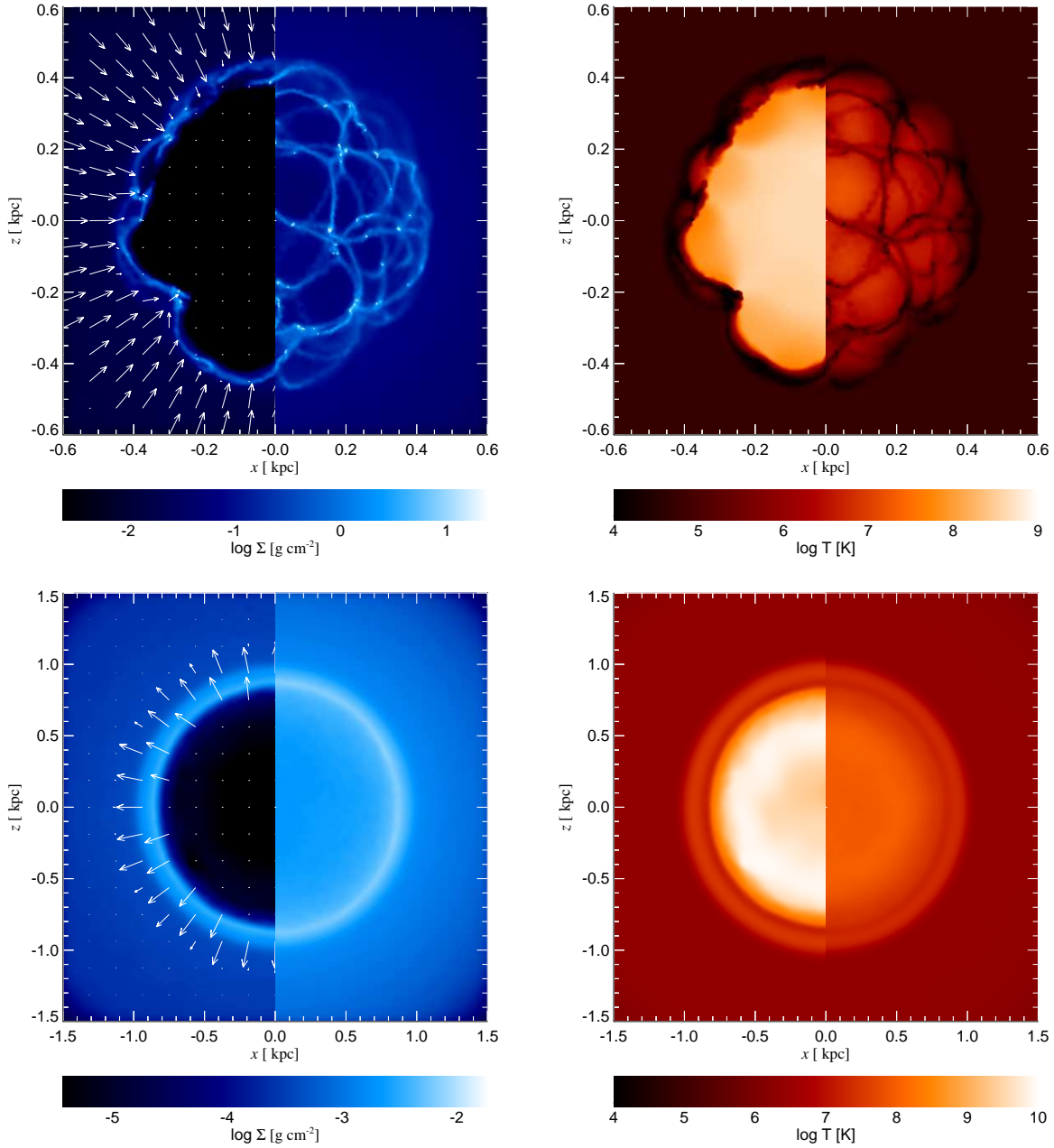


Figure 1. Gas outflows for a gas-rich simulation F1 (top panels) at time $t = 3.8$ Myr (top) and same for a gas-poor simulation F0.03 at $t = 0.57$ Myr (bottom panels). The left panels show projected gas density and the right ones show gas temperature. To expose the 3D nature of the flows, the left sides of each panel show geometrically thin “wedge-slice” projections of the gas flow, where only regions $y^2/(x^2 + y^2 + z^2) < 1/16$ are shown; the right-hand sides of the panels show full cube projections. The shell in the gas-rich simulation cools rapidly and becomes unstable to thin shell instabilities (Vishniac 1983). The shell in the gas-poor simulation cools very slowly, and is thus hot and radially extended. This shell is stable and remains spherically symmetric as the gas is driven away.

Cattaneo A., Faber S. M., Binney J., et al., 2009, *Nature*, 460, 213
 Ciotti L., Ostriker J. P., 2007, *ApJ*, 665, 1038
 Di Matteo T., Springel V., Hernquist L., 2005, *Nature*, 433, 604
 Faucher-Giguere C.-A., Quataert E., 2012, *ArXiv e-prints*
 Goodman J., 2003, *MNRAS*, 339, 937
 Häring N., Rix H.-W., 2004, *ApJL*, 604, L89
 Hobbs A., Nayakshin S., Power C., King A., 2011, *MNRAS*,

413, 2633
 King A., 2003, *ApJL*, 596, L27
 King A., 2005, *ApJL*, 635, L121
 King A. R., Pringle J. E., 2006, *MNRAS*, 373, L90
 King A. R., Zubovas K., Power C., 2011, *MNRAS*, 415, L6
 Kormendy J., Bender R., Cornell M. E., 2011, *Nature*, 469, 374
 Mac Low M.-M., McCray R., Norman M. L., 1989, *ApJ*, 337, 141

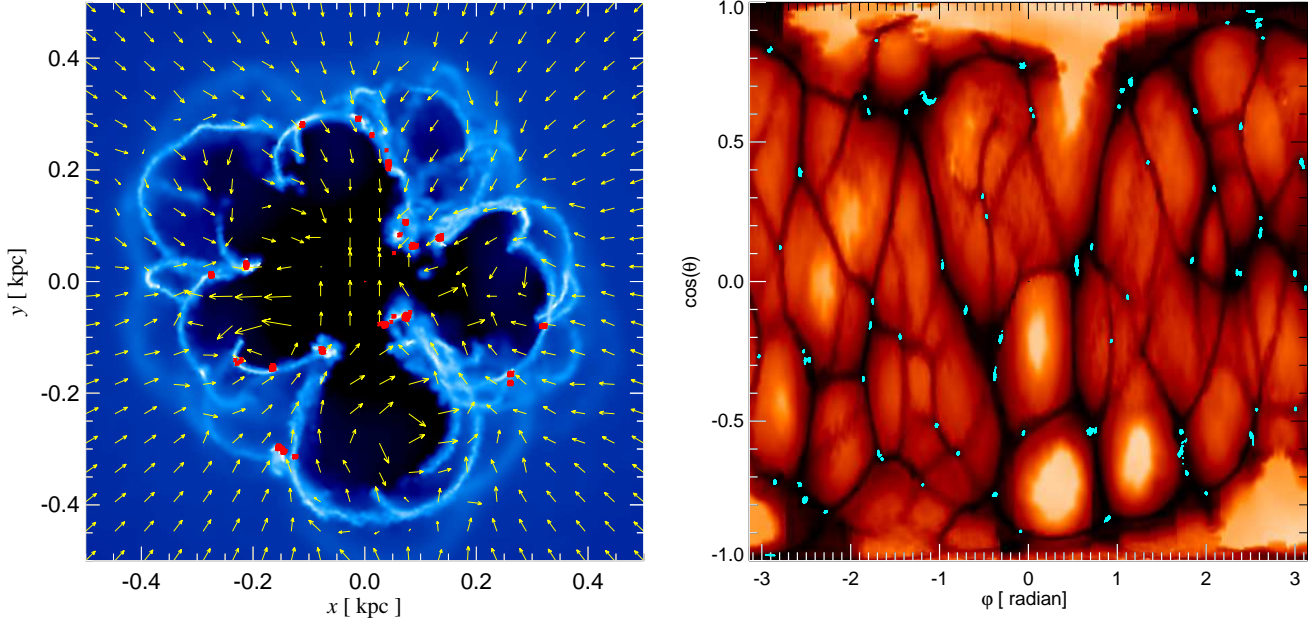


Figure 2. Left panel: “Wedge projection” (see fig. 1) of gas density and velocity vectors for simulation F1 at time $t = 5.2$ Myr. The high density regions of the shell receive less quasar feedback per unit mass and thus fall inward. Red symbols show newly born stars that form within the dense filaments. Most of the stars form in clusters which are disrupted when passing through the central regions of the galaxy. Right panel: Temperature of the gas as seen from the SMBH, averaged along rays, for a shell $0.2 < r < 0.4$ kpc, at time $t = 4.3$ Myr, and as a function of the two spherical angles in spherical coordinates, defined in the usual way: $\cos \theta = z / \sqrt{x^2 + y^2 + z^2}$, and $\sin \phi = y / \sqrt{x^2 + y^2}$. Cyan symbols show locations of the stars. These form exclusively inside the density peaks (corresponding to minima in temperature), which occur most frequently at the intersections of the filaments. The colour scales for the panels are same as they are in figure 1 for simulation F1.

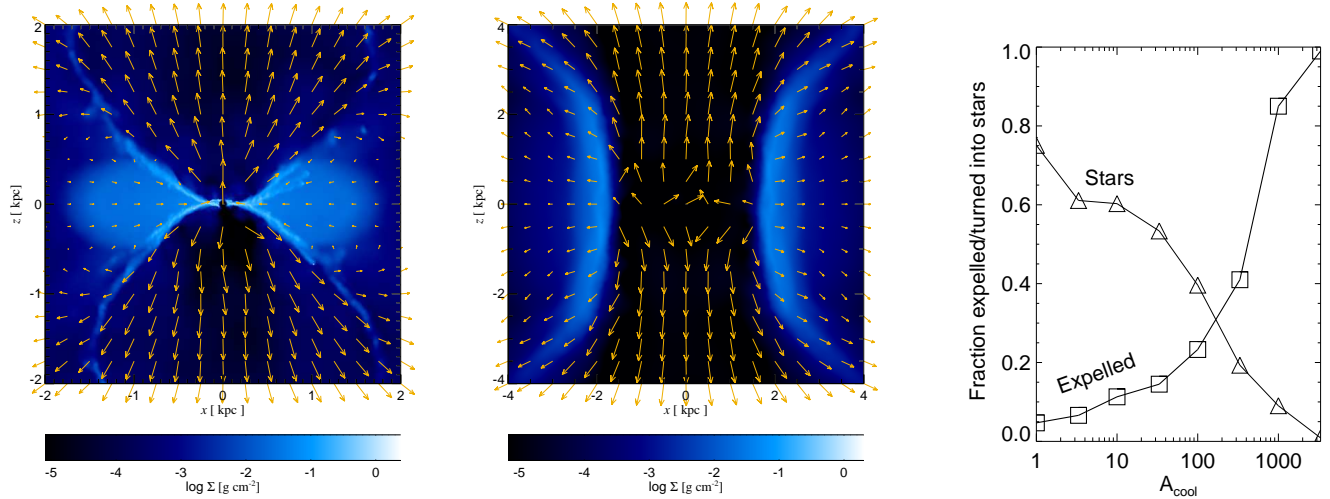


Figure 3. Quasar feedback on an initially elliptically-shaped and slowly rotating shell in the cases with the proper radiative cooling on for the shocked gas (left panel) and for the case when radiative cooling is switched off (middle panel). In both cases gas is expelled along the vertical direction. However, with cooling on, the gas settles into a high density disc that is resilient to quasar feedback. Very little gas is ejected from the galaxy in this case; most is turned into stars or accreted through the inner boundary condition. In contrast, with cooling off, all of the ambient gas is expelled to infinity because no high density features form; hot and diffuse gas is much more susceptible to quasar feedback. The right panel shows how the fraction of the shell expelled to infinity and turned to stars at the end of the simulations ($t = 9$ Myr) change as radiative cooling is progressively suppressed by factor A_{cool} (the left panel corresponds to $A_{\text{cool}} = 1$, and the middle panel to $A_{\text{cool}} = \infty$). More and more gas is ejected rather than turned into stars as cooling is suppressed.

- Nayakshin S., Cha S.-H., Hobbs A., 2009, MNRAS, 397, 1314
- Nayakshin S., Cuadra J., Springel V., 2007, MNRAS, 379, 21
- Nayakshin S., Power C., 2010, MNRAS, 402, 789
- Nayakshin S., Power C., King A. R., 2012, ArXiv e-prints
- Paczynski B., 1978, Acta Astron., 28, 91
- Pounds K. A., King A. R., Page K. L., O'Brien P. T., 2003a, MNRAS, 346, 1025
- Pounds K. A., Reeves J. N., King A. R., Page K. L., O'Brien P. T., Turner M. J. L., 2003b, MNRAS, 345, 705
- Power C., Nayakshin S., King A., 2011, MNRAS, 412, 269
- Sazonov S. Y., Ostriker J. P., Ciotti L., Sunyaev R. A., 2005, MNRAS, 358, 168
- Schawinski K., Lintott C. J., Thomas D., et al., 2009, ApJ, 690, 1672
- Sijacki D., Springel V., di Matteo T., Hernquist L., 2007, MNRAS, 380, 877
- Silk J., Norman C., 2009, ApJ, 700, 262
- Silk J., Rees M. J., 1998, A&A, 331, L1
- Springel V., 2005, MNRAS, 364, 1105
- Tacconi L. J., Neri R., Chapman S. C., et al., 2006, ApJ, 640, 228
- Thompson T. A., Quataert E., Murray N., 2005, ApJ, 630, 167
- Tombesi F., Cappi M., Reeves J. N., et al., 2010, A&A, 521, A57+
- Tremaine S., Gebhardt K., Bender R., et al., 2002, ApJ, 574, 740
- Vishniac E. T., 1983, ApJ, 274, 152
- Zubovas K., King A., 2012, ApJL, 745, L34
- Zubovas K., Nayakshin S., 2012, ArXiv e-prints